Free Arrangement Wireless Power Transfer System With a Ferrite Transmission Medium and Geometry-Based Performance Improvement

Seoktae Seo, Hyunkyeong Jo, *Student Member, IEEE*, and Franklin Bien, *Senior Member, IEEE*

***Abstract*—A free arrangement wireless power transfer system with a ferrite transmission medium and geometry-based performance improvement method are introduced here. The proposed system addresses the efficiency collapse caused by misalignment or increased distance between the transmitter and receiver coils, that is, receivers can be located anywhere on the plate-shaped system, which can be applied to a table, wall, or floor to supply electrical power as needed. Despite its high cost, ferrite is advantageous over air as a medium as the latter diminishes the efficiency at a distance or misalignment. Further, ferrite reduces the transmitter volume and number of coil turns, which is useful for practical applications. Skewed-shape coil windings with higher effective mutual inductance than unskewed structures are used in this system to increase power transfer efficiency. The improvements from the ferrite and coil-winding geometry are verified through Ansoft Maxwell v14.0 and MATLAB simulations. Four prototypes of the proposed system are fabricated and validated at 100 kHz. The highest transfer efficiency at the farthest distance, 55 cm, is 17.5% with the 4-cm-skewed ferrite structure, whereas no power is delivered beyond 10 cm in air. Consequently, the proposed system achieves wider power transfer area and better efficiency without additional power and coil windings while the system complies with the guidelines provided by International Commission on Non-ionizing Radiation Protection (ICNIRP) and IEEE for human safety. This article is accompanied by a demonstrating video.**

***Index Terms*—Coil winding, ferrite, wireless power transmission.**

Manuscript received April 25, 2019; revised June 27, 2019 and August 16, 2019; accepted September 22, 2019. Date of publication October 3, 2019; date of current version February 11, 2020. This work was supported in part by the MSIT (Ministry of Science and ICT), Korea, under ITRC (Information Technology Research Center) support program (IITP-2019-2017-0-01635) supervised by the IITP (Institute for Information & communications Technology Promotion), in part by NRF (National Research Foundation) Grant funded by the Korean Government (NRF-2017-Fostering Core Leaders of the Future Basic Science Program/Global Ph.D. Fellowship Program), and in part by Basic Science Research Program through the National Research Foundation of Korea (NRF) funded by the Ministry of Science and ICT (NRF-2017R1A5A1015596). Recommended for publication by Associate Editor J. Acero *(Corresponding author: Seoktae Seo.)*

The authors are with the School of Electrical and Computer Engineering, Ulsan National Institute of Science and Technology, Ulsan 44919, Korea (e-mail: seoktae333@unist.ac.kr; johk@unist.ac.kr; bien@unist.ac.kr).

This article has supplementary downloadable multimedia material available at http://ieeexplore.ieee.org provided by the authors. This includes an MP4 Video, which demonstrates "Free arrangement WPT system". This material is 139 MB in size.

Color versions of one or more of the figures in this article are available online at http://ieeexplore.ieee.org.

Digital Object Identifier 10.1109/TPEL.2019.2945532

I. Introduction

WIRELESS power transfer (WPT) topology, demonstrated by Nikola Tesla a century ago [1], solves the problems associated with using a power cable, namely the limitations of direct connection, device placement, cable replacement costs, risk of electric shock, and aesthetic point of view. For these reasons, WPT systems have been widely used in biomedical implants, electric vehicles, railway vehicles, underwater vehicles, rescue robots, sensor charging, and portable electronics [2]–[15]. Notably, WPT systems are used to charge mobile devices and provide convenience to those who need to charge these devices frequently in cases of increased power consumption due to surges in data usage. The performance of conventional WPT systems comprising two or four coils with air medium is, however, severely affected by two main factors: alignment and distance between the transmitter (Tx) and receiver (Rx) coils [16]–[18]. When misalignment occurs or charge distance increases, power transfer efficiency is reduced significantly [16]. Consequently, studies have been conducted to extend the transfer distance and create a flexible power path beyond the general structure of WPT systems [16], [19]–[28].

Planar wireless charging platform technologies, which is one of the solutions of abovementioned problem, can be classified as: 1) horizontal flux approaches and 2) vertical flux approaches [22]. In the former, the magnetic flux is generated parallel to the charging surface and the vertical surface area perpendicular to the lines of flux is required to obtain power. If the plane of the vertical surface area is in the same direction of the flux, no energy is transferred to the Rx coils. Therefore, the vertical surface requirement (i.e., the requirement of the area perpendicular to the charging surface) can impose certain impractical restrictions on the orientation and size of receivers. In contrast, in the vertical flux approach, multiple receivers can be placed freely. The Tx coil arrays, however, generate an enhanced magnetic flux perpendicular to the charging surface, raising safety concerns owing to the increased specific absorption rate (SAR), which could harm the human body [29]–[33].

Zhong *et al*. [16] were the first to propose analysis for a wireless power circular domino-resonator system with noncoaxial axes. As the system involves many domino resonators between the Tx and Rx coils, it presents advantages with regard to an

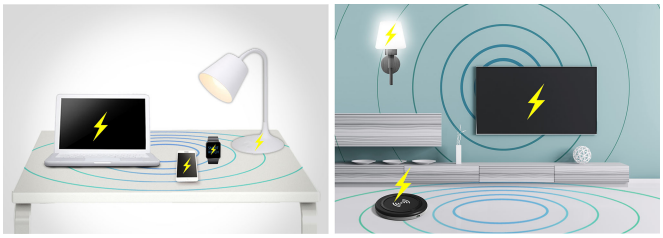

Fig. 1. Expected applications of free arrangement wireless power transfer system with plate structure.

extensible and a bendable power path. A ball-joint WPT system has been used to implement an omnidirectional charging path with ball-shaped movable mechanical parts [28]. However, the position of the Rx coil was restrictive in both the abovementioned studies. In circular domino-resonator systems, which have multiple coils, a particular resonator bears the load to ensure high efficiency [16]. The ball-joint structure described in [28] is a mechanical constraint in itself as the ball and socket, where the coils are embedded, cannot be separated from each other.

Choi *et al*. [27] suggested using a three-dimensional (3-D) charging zone to which power is delivered regardless of the location or direction of the receiver. Air, rather than ferrite, which is a magnetic material, is used as the medium, and it helps obtain an economical system with a uniform magnetic field. However, such an arrangement results in the system having a number of coil turns compared to the transmission distance; low magnetic couplings between the Tx and Rx coils, causing very low peer to peer efficiency; and difficulty in implementation of application due to large transmitter and receiver volumes.

This article presents a WPT system with a plate-shaped power transmission medium as a combination of the horizontal and vertical flux approaches, allowing the receiver to be freely located. This system can be applied to a table for charging mobile devices or to a wall and floor to supply electrical power to home appliances (Fig. 1). Ferrite in the form of a plate is used as the power transmission medium in this system. The medium with a high permeability value concentrates the magnetic field so that high coupling between the Tx and Rx coils is achieved even with a small number of coil turns. The WPT system becomes less sensitive to the alignment between the Tx and Rx coils and reduces volume occupancy for practical applications because of its greatly enhanced efficiency due to high coupling. Through a simulation with finite element analysis (FEA, Ansoft Maxwell v14.0) and MATLAB software and experimental measurements, this study verified the improvement in mutual inductance (an indicator of coupling) and power transfer efficiency when ferrite is adopted as the medium rather than air. In Section II, the overall design elements of the proposed system are studied and determined via analysis and experiments. In Section II.A, in detail, the main features of the proposed system, namely the material of medium, plate-shaped configuration, and winding scheme of the Tx coil, are designed based on the three methods: 1) increasing the number of coil turns; 2) changing the material of the medium; and 3) employing a new system structure) to compensate the decrease in efficiency under misalignment conditions. Section II.B provides the three design criteria and the reasons behind their selection based on the utility, feasibility, and safety of application. The parameters of the structure, such as specific dimensions and the number of coil turns, are provided in the section. In Section III, a geometry-based performance improvement method with a skewed coil structure involving no additional windings or cost is proposed to increase the mutual inductance between the Tx and Rx coils. The enhancement of power transfer efficiency is verified via simulations using the aforementioned softwares and experimental measurements. The modification of the coil winding is based on the structural theory of the WPT system. The transfer efficiency is observed to confirm the improved performance of the proposed arrangement through a power transfer experiment at 100 kHz, using a fabricated free arrangement WPT system with a ferrite plate of dimensions 30 $\times$ 70 cm. Finally, the conclusions are presented and directions for future work are defined as studies covering multiload charging and very large charging areas.

II. Free Arrangement Wireless Power Transfer System With Ferrite Medium

A. Configuration of the Proposed Free Arrangement Wireless Power Transfer System

A WPT system with a plate structure proposed in Fig. 2 can conveniently charge a receiver irrespective of its location on the plate. A Tx coil, to which an ac power source provides electrical power, is tied to one edge of the large plate. An Rx coil receiving the power for the load and wound with the Rx box is freely located on the surface of the plate. A load can be any electrical device that is directly power-supplied or a battery that needs to be charged. This arrangement can solve serious problems encountered when using conventional wireless battery chargers, namely, severe sensitiveness to alignment between coils and very short charging distance, which originates from their structures and underlying principles, as explained in the following paragraph. These limitations can be solved by creating a system that allows free arrangement of the receiver on the power transmission medium plate.

The principle followed by conventional wireless battery chargers is shown in Fig. 3. When ac current (I) flows from the power source to the Tx coil, magnetic field is induced around the coil due to Ampere's law (1). This field propagates into the Rx coil through air. Time-varying magnetic flux density (B), transformed from magnetic field intensity (H) in the Rx coil, induces a voltage difference between the ends of the load as per Faraday's law (2). During the process, electrical power in the form of the magnetic field is transferred from the Tx coil to the Rx coil

$$\oint \vec{H} \cdot d\vec{l} = \vec{I} \tag{1}$$

$$\int \vec{E} \cdot d\vec{l} = -\frac{\partial}{\partial t} \int \vec{B} \cdot d\vec{S}. \tag{2}$$

The higher the magnetic field linked to the Rx coil, the higher the power transfer efficiency at the same supplied power. If the lateral distance (d_{lateral}, which is associated with the alignment issue) or longitudinal distance ($d_{\mathrm{longitudinal}}$, which is associated

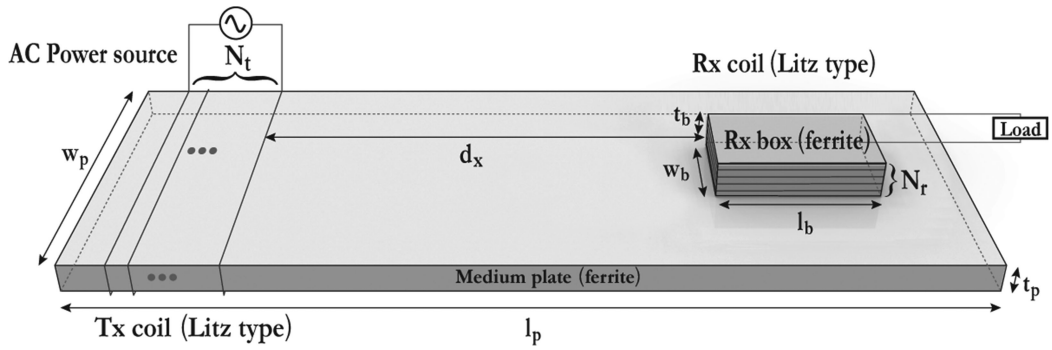

Fig. 2. Proposed novel structure of the free arrangement wireless power transfer system.

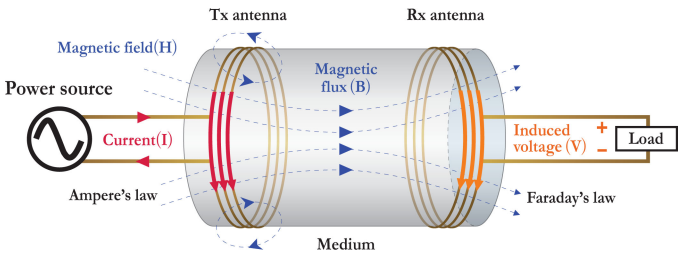

Fig. 3. Principle of conventional wireless power transfer model.

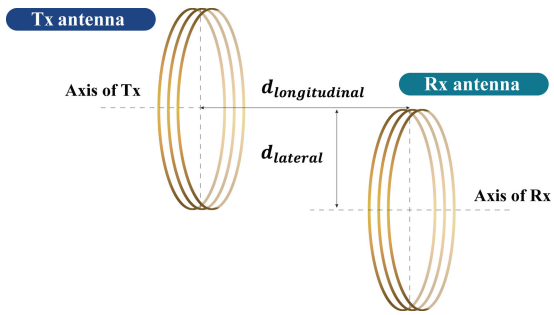

Fig. 4. Lateral and longitudinal distances between the transmitter and receiver coils.

with the charging distance issue) is increased, as depicted in Fig. 4, the linkage of the magnetic field decays considerably. This implies that the receiver can be charged at a fixed position, and the reduction in efficiency due to the increases in the abovementioned distances leads to extended charging time and heat generation in devices, threatening the user's safety. To overcome these problems, the proposed WPT system utilizes three methods, as presented below.

Power transfer efficiency, under misalignment condition, can be improved by: 1) increasing the number of coil turns; 2) changing the material of the medium; and 3) employing a new system structure in spite of increments in the lateral and longitudinal distances. Because a large number of windings generates a magnetic field proportional to the number of windings, the linkage of the field is strengthened, thus improving efficiency. However, adding the coil turns expands the volume of the transceiver and results in increasing the coil resistances, which reduces efficiency. This is why the relationship between coil turns and efficiency is complicated (discussed in Section II.B in detail). Therefore, the coil turns should be regulated at a certain level.

The second method to increase the efficiency involves using an adequate material as the medium, such that the magnetic field propagates from the Tx coil to the Rx coil. High permeability, a property of the material, guarantees improved efficiency. When the current that flows in the Tx coil generates the magnetic field as per (1), the field is transferred to the Rx coil in the form of the magnetic flux density (B). Because high magnetic flux density ensures that a larger voltage (V) difference is induced on the load (R), as described in (2), it is necessary for the magnetic flux density to be high to achieve high power (P), as per (3), and transfer efficiency

$$P = \frac{V^2}{R}. \tag{3}$$

The relationship between magnetic field intensity (H) and B is as follows:

$$B = \mu_0 \mu_r H \tag{4}$$

where μ_0 and μ_r are permeability of vacuum and material relative to the vacuum. The magnetic field is well transformed into the magnetic flux density if the material of the medium between the Tx and Rx coils has a higher value of permeability than vacuum (Fig. 3). That is, high permeability of a material as a medium induces a concentrated magnetic field in the medium, and hence, the power is transferred with lower loss. Ferrite, a ferrimagnetic material, has very intense relative permeability (in the order of thousands). It is selected as a medium for this reason. Deploying ferrite results in a more expensive system compared with one using air. However, the structure of the proposed WPT system in Fig. 2 cannot be implemented with the desired efficiency using air (as verified by the experiment in Section III). The advantages, such as the fewer coil turns required for the same efficiency and reduction of transmitter volume due to the use of ferrite, besides, can compensate for the cost.

Free arrangement of the receiver for receiving power, the most prominent characteristic of the proposed WPT system, is achieved by designing a new structure, which is referred to as the third method, to ensure high efficiency. Fig. 5 shows the most flexible power paths that can be implemented by a virtual medium linkage between the transmitter and the receivers at arbitrary locations. However, ferrite as a medium cannot be deformed in the manner of fluid; thus, the system with a plate

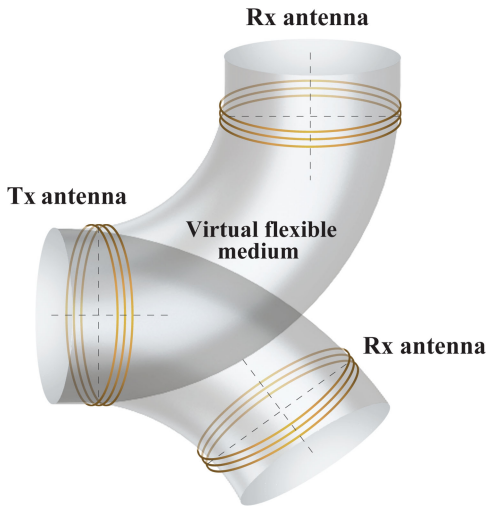

Fig. 5. Flexible power paths between the transmitter and receiver coils with a virtual medium.

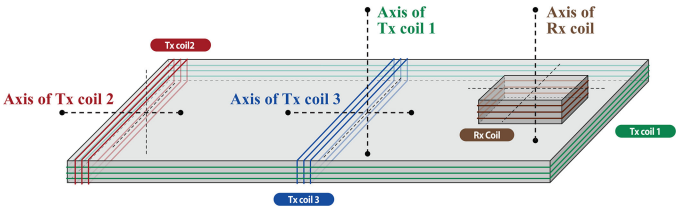

Fig. 6. Various locations of transmitter coils: axis of Tx coils 1 parallel to that of Rx coil (green); axes of Tx coil 2 (red); and Tx coil 3 (blue) perpendicular to that of Rx coil at the edge and at the center of the plate.

structure (shown in Fig. 2) is adopted as a practical design to build the power paths for randomly located receivers. Because the location of the Tx coil also poses an issue in a system with a plate, several winding methods of the Tx coil are suggested in Fig. 6. When a receiver is located on the medium plate, the central axis of the Tx coils can be parallel (Tx coil 1) or perpendicular (Tx coils 2 and 3) to that of the Rx coil. Tx coils 2 and 3 are tied at one edge and center of the medium plate, respectively. Although Tx coil 1 has the strongest magnetic flux linkage to the Rx coil compared with the other windings, it may have lowest efficiency due to very long coil length with the same the number of windings, which involves high resistance. In addition, the strongest magnetic flux can bring controversial issue about safety. Tx coils 2 and 3 have almost identical properties with respect to the flux linkage to Rx and the resistance, except for the possible propagation distance. Consequently, the winding method described as Tx coil 2 in Fig. 6 is determined to be used for the proposed system because power transfer efficiency at the maximum number of available medium plates should be experimentally verified.

Typical operating frequencies used for the WPT are 20 kHz, 60 kHz, 100 kHz, and 6.78 MHz. The higher the frequency, the larger the voltage difference generated between the load, and hence, more power is delivered. However, an increase in wire resistance due to the skin effect and magnetic loss at high frequency (over the order of 1 MHz) are known to occur [34].

TABLE I
STRUCTURAL PARAMETERS OF THE FREE ARRANGEMENT WIRELESS POWER TRANSFER SYSTEM

Structure parameter	Symbol	Value
Length of medium plate	l_p	70 cm
Width of medium plate	w_p	30 cm
Thickness of medium plate	t_p	0.5 cm
Length of receiver box	l_b	5 cm
Width of receiver box	w_b	5 cm
Thickness of receiver box	t_b	0.5 cm
Operating frequency	f	100–105 kHz
Type of wire	·	Litz wire
Material of medium	·	Ni–Zn type soft ferrite material, SN-20 (Samwha Electronics, Korea)

Hence, the proposed WPT system is designed to operate at 100 kHz.

B. Consideration of Design Variables for Free Arrangement Wireless Power Transfer System

Certain design elements should be determined to verify the feasibility and performance of a free arrangement WPT system, namely dimensions of the medium plate and Rx box, type of wire, and number of coil turns. The dimensions of the medium plate and receiver box are decided by considering the available material (Ni-Zn-type soft ferrite material SN-20 acquired from Samwha Electronics, Korea) and applications in Fig. 1. Considering the most desired application, a simultaneous charging pad for several mobile devices, the area to be covered is set to approximately 30×50 cm^2. The length of the medium plate, including the volume of the transmitter, is selected as 70 cm. The dimensions of the Rx box are also determined based on the applications for mobile devices, as listed in Table I. The Litz wire, which is used as a coil, is adequate for high operating frequency. ac wire resistance owing to the skin effect increases as the system works at high frequency. The Litz wire, which is composed of several bundles of wire, is employed as it attenuates the ac resistance.

The numbers of Tx and Rx coil turns should be investigated thoroughly because they are closely related to the efficiency of transferred power. The efficiency is one of the most important indicators to evaluate the performance of the system. Therefore, an analysis of the efficiency is conducted based on the circuit model of the system to devise a guideline for the number of coil turns.

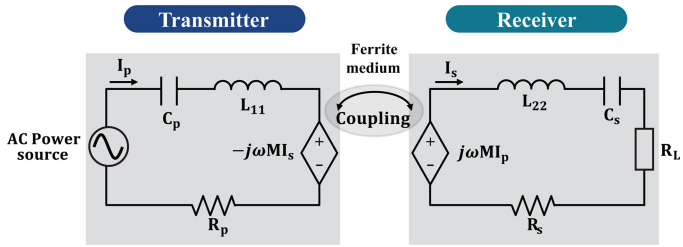

Fig. 7. Circuit modeling of the free arrangement wireless power transfer system.

Fig. 7 shows a basic circuit model of a WPT system with ferrite medium. The current flowing through the primary coil, denoted as primary current (I_p) in Fig. 7, is supplied from the power source, and secondary current (I_s) flows through the secondary coil. Coil resistance and self-inductances of the Tx and Rx coils $(R_p, R_s, L_{11}, \text{ and } L_{22})$ are measured using a network analyzer (E5061B, Keysight Technologies). By adding compensating capacitors $(C_p \text{ and } C_s)$ for resonance with self-inductances, high power transfer efficiency can be achieved. The load of receiver is R_L. The effective mutual inductance (M) expresses the coupling between the coils and the medium where the magnetic flux is induced. When $\omega\ (= 2\pi f)$ is the operating angular frequency, power transferred to the receiver and power reflected by Lenz's law are expressed by $j\omega MI_p$ and $-j\omega MI_s$, respectively. The power transfer efficiency (η) is formulated as

$$\eta = \frac{R_L}{(R_s + R_L)\left(1 + \frac{R_s + R_L}{(\omega M)^2} R_p\right)}. \tag{5}$$

As per (5), that high efficiency results in low coil resistances (R_s and R_p) and high mutual inductance (M). The resistances are proportional to the lengths of the coils. The mutual inductance increases as the number of coil turns increases, because a higher number of coil turns generates a stronger magnetic field in the medium plate, ensuring enhanced coupling between the Tx and Rx coils. The number of coil turns should have some constraints, not only because of the tradeoff between the resistances and the mutual inductance but also to ensure feasible applications. As it is excluded from the charging zone, the area occupied by the transmitter is restricted to 15% of the transfer medium plate, which measures $30 \times 70\ \text{cm}^2$. Also, the Rx coils, which can be implanted to the mobile device, should have as small a size as possible. Therefore, the following three design criteria are suggested to select the appropriate number of coil turns, considering feasibility and safety:

1) Maximum coil turns in a limited area;
2) Maximum average transfer efficiency;
3) Maximum efficiency at a distance of 50 cm.

To choose the proper number of coil turns, an experiment to measure the efficiencies of different numbers of coil turns is conducted. Fig. 8(a), (b), and (c) depict the experimental results of power transfer efficiency with different Tx coil turns (20, 30, and 40), and two types of Rx coil windings (10 and 15 turns) are used regardless of the number of Tx coil turns. Rx boxes with over 15 turns of coils cannot meet design criterion 1) because of the physically unimplementable structure. Tx coils with over 40 turns are also excluded from consideration as improvement in the overall efficiency is not observable due to the tradeoff between the resistances and the mutual inductance. The efficiency for each case is measured by varying the distance between the Tx and Rx coils (d_x), because the Rx coil can be placed on the whole medium plate surface. The system design variables for the experiment are listed in Table I. Usually, higher efficiency is observed as the receiver gets closer to the Tx coil, that is, with small d_x, and vice versa. The efficiencies are always higher at 15 Rx turns than at 10 turns. The configuration (maximum, average, and at-50-cm) of efficiencies with 30 Tx turns is similar to that for 20 turns because the mutual inductance of the system with 30 turns does not considerably increase over that of 20 turns; however, primary resistance does.

The combination of 40 Tx and 15 Rx turns has the best performance at any location. The maximum, average, and at-50-cm efficiencies of the combination are 29.5%, 12.7%, and 5.8%, respectively. Even though the Rx coil of 10 turns with 40 Tx turns shows an efficiency close to the best combination at 50 cm, the average efficiency cannot exceed 10%. Efficiencies at different distances (d_x) for 40 Tx turns and 15 Rx turns increase by more than 1.3 times on average than for those with 40 Tx turns and 10 Rx turns. Based on the design criteria, the numbers of coil turns are chosen as 40 turns for the Tx and 15 turns for the Rx coils.

III. Free Arrangement Wireless Power Transfer With Geometry-Based Performance Improvement

A. Relationship Between Mutual Inductance and Power Transfer Efficiency

The close relationship between mutual inductance and power transfer efficiency is investigated. The previous section showed that the increase in the number of coil turns does not directly improve the efficiency because both resistances and mutual inductances increase. The number of Tx and Rx coil turns is determined to be 40 and 15 through the former experiments measuring the efficiency for different combinations of coil turns, and the electrical parameters are denoted in Table II. The resistances with the fixed number of coil turns are deterministic, so that the effect of the mutual inductance alone on the efficiency is considered. The mutual inductance cannot be measured directly; the value must be estimated. Fig. 9 shows the circuit model of the WPT system without resistive load. V_R is the induced voltage between the two ends of the Rx coil and the secondary current, I_s, is negligible owing to the almost infinite resistance of the open circuit. When power is supplied from the source to the Tx, primary current, I_p, flows normally, and then, the voltage on Rx is calculated using

$$V_R = j\omega MI_p. \tag{6}$$

Mutual inductance is estimated by measuring V_R and I_p.

In Fig. 10, the orange and blue lines depict power transfer efficiency from the simulation and experiments, respectively.

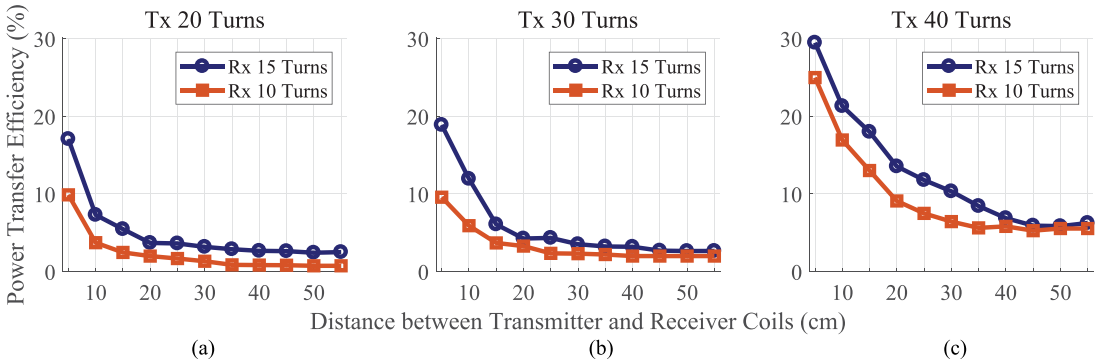

Fig. 8. Experimental results of power transfer efficiencies by varying the distance between the two coils with (a) 20 Tx coil turns, (b) 30 Tx coil turns, and (c) 40 Tx coil turns, and two different turns of the Rx coil (10 and 15).

TABLE II
FIXED NUMBER OF TX AND RX COIL TURNS AND OTHER PASSIVE ELECTRICAL PARAMETERS FOR A FIXED NUMBER OF WINDINGS

Design parameter	Symbol	Value
Number of transmitter coil turns	N_t	40
Number of receiver coil turns	N_r	15
Resistance of transmitter coil	R_p	12 Ω
Resistance of receiver coil	R_s	0.48 Ω
Self-inductance of transmitter coil	L_{11}	995 μH
Self-inductance of receiver coil	L_{22}	63 μH
Compensating capacitance of transmitter coil	C_p	2.5 nF
Compensating capacitance of receiver coil	C_s	40.4 nF
Load resistance	R_L	0.5 Ω

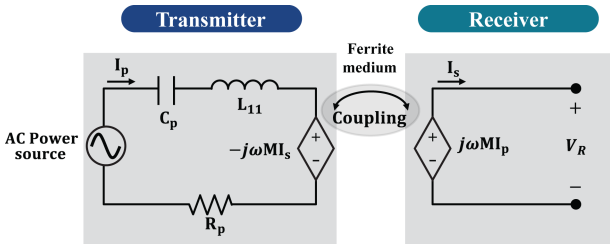

Fig. 9. Basic circuit model of wireless power transfer system without load.

The simulation is conducted in MATLAB software (R2017a) using the measured mutual inductance from the abovementioned method and (5). The efficiencies are obtained by moving the receiver from the Tx coil when the distance between the two coils varies from 5 to 55 cm.

The correlation between the simulated and measured efficiencies is verified using R^2, the coefficient of determination. R^2 is

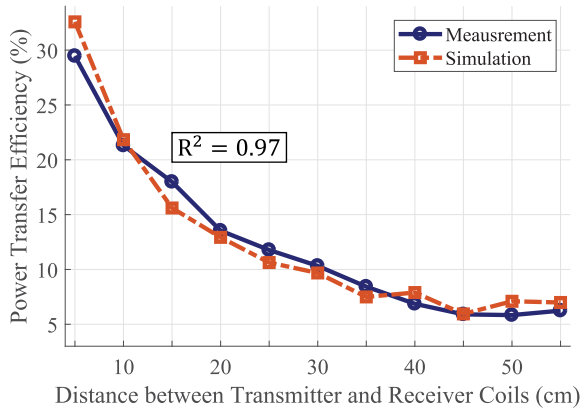

Fig. 10. Power transfer efficiency of the simulation (orange dashed line) and experiment (blue solid line) for 40 Tx coils and 15 Rx coils by varying the distance between the Tx and Rx coils.

a statistical value that is used to test the hypothesis and shows how well the observed data follow the prediction, depicted by a value between 0 and 1 [35], [36]. The measured points are better replicated by the model; further, R^2 tends to unity. In Fig. 10, the R^2 value of 0.97 (that is very close to unity) confirms that the simulation of the power transfer efficiency is well modeled and estimates the outcomes with high accuracy.

B. Analysis of Effective Mutual Inductance

High power transfer efficiency requires high mutual inductance, which means the intensity of magnetic field inside the Rx coil should be sufficiently high based on (2)–(4). In the structure proposed previously, however, a low net intensity of the magnetic field is observed because the magnetic fields induced by the upper and lower parts of the Tx coil have similar intensities as well as opposite directions, as shown in Fig. 11. Since the induced magnetic fields offset each other, the effective mutual inductance that shows linkage between the Tx and Rx coils appears to be low. In order to increase the effective mutual inductance, the difference between the intensity of the magnetic field induced by the upper and lower Tx coils should be increased.

The magnetic field in the proposed system is weak as the opposite directions of the currents flowing in the upper and lower Tx coils induce a field in the opposite direction in the Rx box,

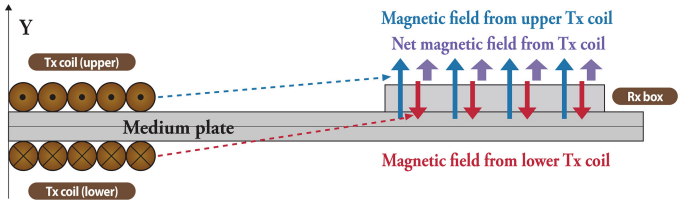

Fig. 11. Difference in the magnetic field (purple arrows) induced by the upper (blue arrows) and lower parts (red arrows) of the transmitter coil.

based on Ampere's right-hand rule (1), whereas the intensity that depends on the distance is comparable. If the Tx coil is skewed, as shown in Fig. 12, and the influence of the upper part of the Tx coil on the Rx coil (emerald and green arrows on Rx coil in Fig. 12) is relatively stronger than that of the lower part (red arrow on Rx coil in Fig. 12), the effective mutual inductance will increase as the intensity difference of the magnetic field induced by the two elements increases.

The feasibility of the proposed method, namely adjusting the winding structure of the Tx coil, is verified with FEA simulation (Maxwell v14.0) and depicted in Figs. 13 and 14. Fig. 13(a) shows the entire model of the system and magnetic flux density in the ferrite plate. A high magnetic flux density (22.73 mT), exceeding the safety standard, is induced; this is acceptable because electrical power is transferred through the ferrite plate in the form of a magnetic field. The *x*-*y* plane that obtains the strongest induced magnetic field touches the Tx coil (Fig. 13(b)). Fig. 13(c) presents the magnetic field of the *y*-*z* plane 1 cm from the Tx coil. Fig. 13(d) shows the simulation result of the *z*-*x* plane at y = 15 cm. The magnetic flux density results of Fig. 13(b), (c), and (d) decrease significantly as the distance of the measurement point from the coil increases.

The simulated vaues are compared after normalization with the maximum value, which is obtained from a 4-cm-skewed Tx coil, because of uncertainty in the permeability of the ferrimagnetic material. The system with the 2-cm-skewed Tx coil has twice as high normalized mutual inductance on average compared to that with the unskewed Tx coil. It is certain that the most deformed Tx coil shows the best performance, presenting over five times higher mutual inductance on average than that with the conventional Tx coil.

Based on this verification, this article introduces a geometry-based performance improvement method, which can increase the effective mutual inductance between the Tx and Rx coils by adjusting the winding structure of the Tx coil. Adjusting the winding structure can increase mutual inductance easily, which leads to improved transfer efficiency, without considerable additional cost compared to applying a new medium material and increasing the number of coil turns. In the following simulations and experiments, the distance between the Tx and Rx coils (d_x) is defined as the minimum length between the two coils, that is, between the rightmost part of the Tx coil and the leftmost part of the Rx coil; adjusting the Tx coil winding thus does not affect d_x.

Simulations were conducted using MATLAB to verify that the effective mutual inductance between the Tx and Rx coils increases with the increase in skewness of the Tx coil. Three Tx coils of different skew ratios (0, 2, and 4 cm) were modeled in the simulation, as shown in Fig. 12. Since one of the system design criteria is to restrict the size of the transmitter compared to the overall system, including the transmission distance, models in which the Tx coil is skewed by over 4 cm are not considered. Ferrite is thus adopted as the medium of the simulated systems with three kinds of Tx windings. The comparison, an air coil system with the unskewed Tx coil, is also simulated. The system dimensions for the simulations are listed in Tables I and II.

Neumann's formula in (7f) derived from Maxwell's equations is utilized in the simulation to calculate the mutual inductance (M), expressed by circuit coupling in Fig. 9, between the arbitrary structures [28], [37]. The formula can be derived from Biot–Savart's law in (7a), which describes the magnetic flux density (B_1) generated by a constant electric current (I_1) from the Tx coil as follows:

$$\overrightarrow{B_1} = \frac{\mu_0 \mu_r I_1}{4\pi} \oint_{l_1} \frac{d\vec{l_1} \times (\overrightarrow{r_1} - \overrightarrow{r_2})}{|\overrightarrow{r_1} - \overrightarrow{r_2}|^3} \tag{7a}$$

$$\Phi_2 = \int \overrightarrow{B_1} \cdot d\overrightarrow{S_2} = \int (\nabla \times \overrightarrow{A_1}) \cdot d\overrightarrow{S_2} = \oint_{l_2} \overrightarrow{A_1} \cdot d\overrightarrow{l_2} \tag{7b}$$

$$\overrightarrow{A_1} = \frac{\mu_0 \mu_r I_1}{4\pi} \oint_{l_1} \frac{d\vec{l_1}}{|\overrightarrow{r_1} - \overrightarrow{r_2}|} \tag{7c}$$

$$\Phi_2 = \frac{\mu_0 \mu_r I_1}{4\pi} \oint_{l_1} \oint_{l_2} \frac{d\vec{l_1} \cdot d\vec{l_2}}{|\overrightarrow{r_1} - \overrightarrow{r_2}|} \tag{7d}$$

$$\Phi_2 = M_{21} I_1 \tag{7e}$$

$$M_{21} = M = \frac{\mu_0 \mu_r}{4\pi} \oint_{l_1} \oint_{l_2} \frac{d\vec{l_1} \cdot d\vec{l_2}}{|\overrightarrow{r_1} - \overrightarrow{r_2}|} \tag{7f}$$

μ_0 and μ_r are the permeability in vacuum and relative permeability, respectively. The relative permeability is adjusted according to the medium, namely air or ferrite, in this work. $\overrightarrow{dl}_1$ and $\overrightarrow{dl}_2$ are infinitesimal length vectors along coils 1 and 2, respectively. $\vec{r}_{i=1,2}$ is a vector from the common origin of the 3-D space to the infinitesimal length of the corresponding coil, $\overrightarrow{dl}_{i=1,2}$. Φ_2, the magnetic flux in coil 2 (the Rx coil) is derived from contour integral of the magnetic vector potential of coil 1 ($\vec{A}_1$) along coil 2 and is proportional to the current in coil 1. Thus, the mutual inductance between the Tx and Rx coils can be calculated from (7f).

The contour integral in (7f) is related to the inner product of the infinitesimal parts of the Tx and Rx coils, and is normalized by the distance between them. The contours, which are written as $l_{i=1,2}$, are located along the Tx and Rx coils. Therefore, the mutual inductance estimated from the simulation is affected by the material of the medium (μ_r), the configuration of the Tx and Rx coils ($\overrightarrow{dl}_1 \cdot \overrightarrow{dl}_2$), and the distance between the coils ($|\overrightarrow{r_1} - \overrightarrow{r_2}|$) only.

The results of the simulation in Fig. 15 show that the effective mutual inductances of the systems with ferrite medium remain high even for long distances compared to the conventional WPT system with air medium (purple dashed line with + markers

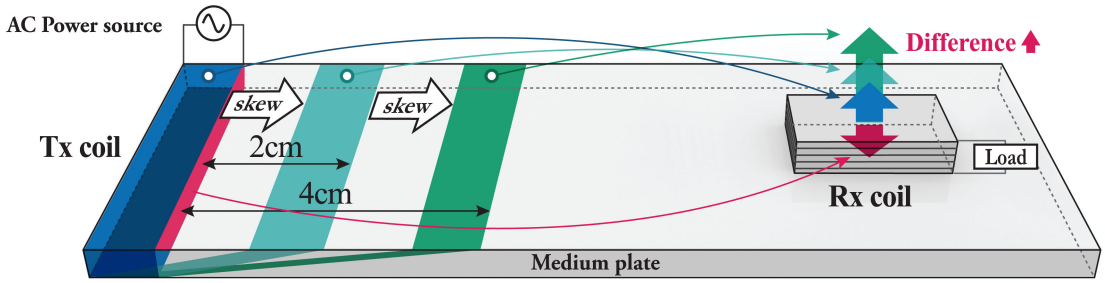

Fig. 12. Proposed performance improvement method with the skewed winding structures of the transmit coil which have different skew levels: unskewed (blue); 2 cm (emerald); and 4 cm (green).

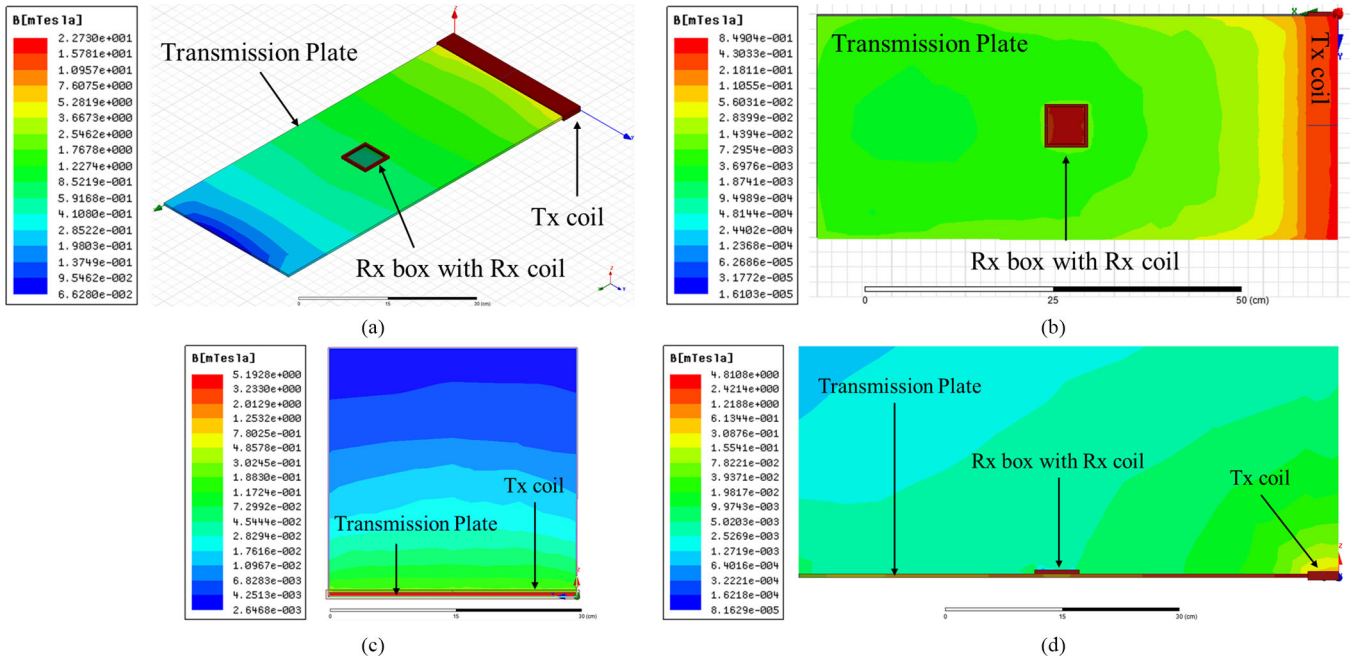

Fig. 13. Results of FEA simulation (Maxwell v14.0) of the system with unskewed Tx coil (a) for the ferrite plate, (b) for the *x*-*y* plane above the Tx coil, (c) for the *y*-*z* plane 1 cm from the coil, and (d) for the *z*-*x* plane in the center of the coil.

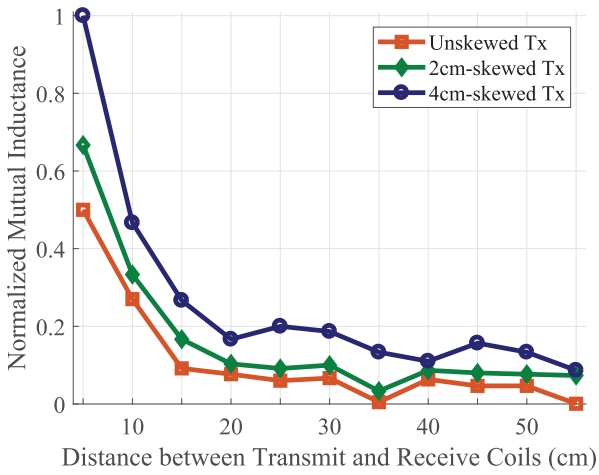

Fig. 14. Simulation result using the Maxwell model to verify the improvement in mutual inductance by adjusting Tx coil winding.

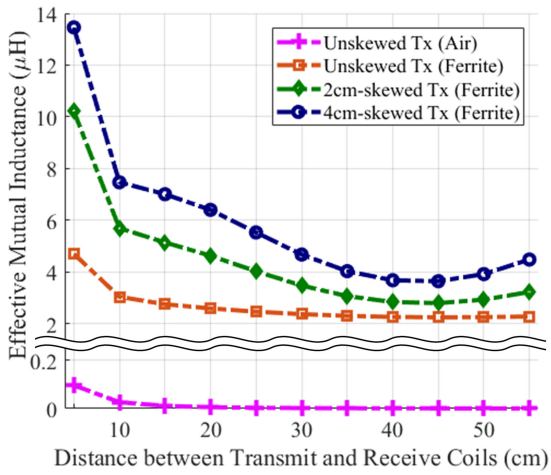

Fig. 15. Simulation result of the relationship between the effective mutual inductance and the skew level of the Tx coil (using MATLAB).

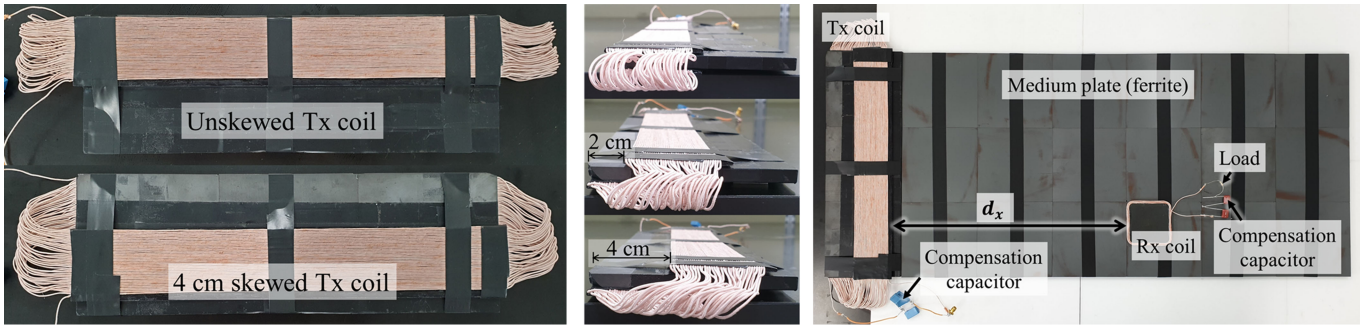

Fig. 16. Prototypes of the unskewed coil and skewed coil structures: (a) top view and (b) side view. (c) Experimental setups with ferrite media.

in Fig. 15), regardless of the winding structure of the Tx coil. The system with air medium shows under 10 nH of mutual inductance at a distance of 10 cm between the Tx and Rx coils. On the other hand, the mutual inductance of the system with ferrite media and the unskewed Tx coil is over 2.2 μH even at a distance of 55 cm and the values with the skewed Tx coils are much higher. It is clear that although the mutual inductance attenuates as the distance between the Tx and Rx coils increases, the power can be delivered for a longer distance using the high-permeability medium compared to the conventional way through air. Further, consistent with the hypothesis, the result of the model with the highest skew level (4 cm) indicates that the improvement in effective mutual inductance raise the transfer efficiency, thus showing the possibility of performance improvement with the winding adjustment of the coil in the system.

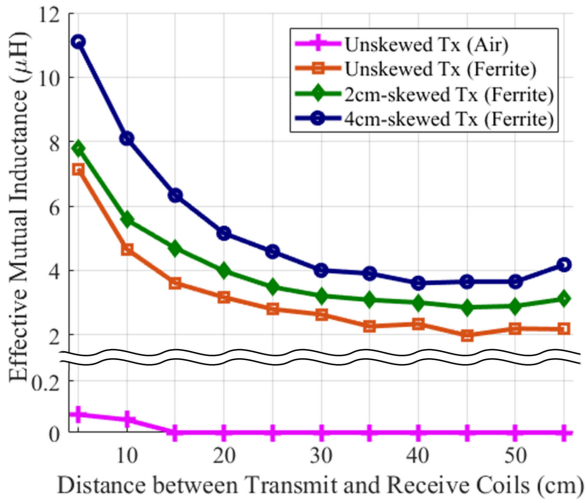

Fig. 17. Experimental result of the relationship between the effective mutual inductance and the skew level of the Tx coil.

C. *Verification of Geometric-Based Performance Improvement (GBPI) Method via Experiments*

The free arrangement WPT systems with unskewed and skewed coil structures (2 and 4 cm) are fabricated as seen in Fig. 16(a) and (b), and practical verification using ferrite medium is completed as seen in Fig. 16(c). Fig. 16 show that only 6.1%, 9.0%, and 11.8% of the system volume are occupied by the transmitter in case of the unskewed, 2-cm-skewed, and 4-cm-skewed structures, respectively, not against the design rules in Section II.B. Each case uses a compensating capacitor to form a tank circuit with a resonant frequency similar to the operating frequency. Since the secondary current should be negligible to measure the effective mutual inductance, the load is linked to the Rx box in series with the compensation capacitors when measuring the transfer efficiency.

Fig. 17 shows the measured effective mutual inductances according to the position of the Rx coil with different skew levels (0, 2, and 4 cm). The mutual inductance with the unskewed structure through air is also measured for comparison with that of the system with ferrite medium. Both simulations (Fig. 15) and measurements (Fig. 17) indicate that the system with ferrite has higher mutual inductance, implying the improved performance in transfer efficiency of the free arrangement WPT system with ferrite. The experimental results are well predicted from the simulations, and the tendencies of the simulated and measured mutual inductances are consistent, providing an R^2 value over 0.94 between the curves for ferrite in Figs. 15 and 17 (0.965, 0.971, and 0.945 for the unskewed with ferrite, 2 cm skewed with ferrite, and 4-cm-skewed with ferrite structures, respectively).

In case of air, regardless of the tendency of the curves to appear similar, the correlation between predicted and observed data is relatively low compared to the cases for ferrite, for a coefficient of determination of 0.835. This can be a possible reason for the relatively low correlation through air when the secondary voltage, which is used to calculate the effective mutual inductance, is too low to be precisely measured over a distance of 15 cm.

In case of the mutual inductance measured in the ferrite system, it is evident that it increases as the Tx coil is further distorted. The maximum effective mutual inductance is 11.1 μH when the 4-cm-skewed Tx coil is 5 cm apart from the Rx coil on the ferrite plate. In the identical system, mutual inductance of 4.18 μH is recorded at a distance of 55 cm, where the distance between the Tx and Rx coils is the largest.

The simulated and measured power transmitter efficiencies of the proposed system according to the receiver locations

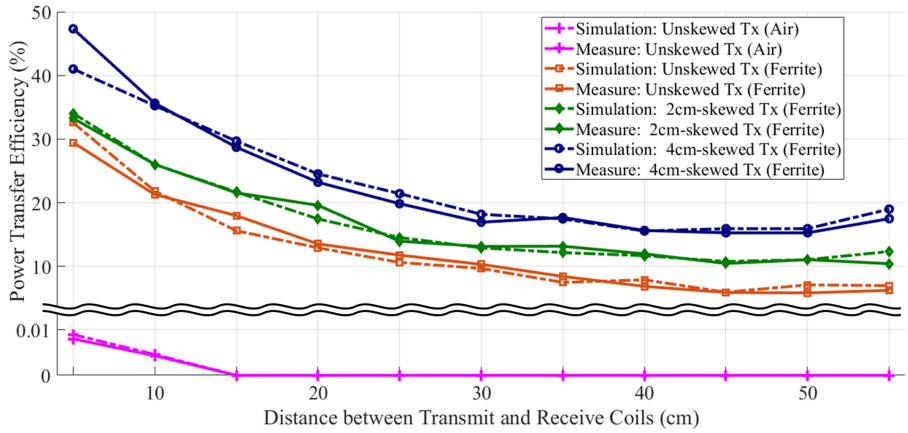

Fig. 18. Simulated and measured transfer efficiencies of the free arrangement wireless power transfer system.

are shown in Fig. 18 for four conditions: unskewed coil with air medium (pink); unskewed coil on ferrite plate (orange); 2-cm-skewed coil on ferrite plate (green); and 4-cm-skewed coil on ferrite plate (blue). The simulation results and measured values are depicted with the dashed and solid lines, respectively. An ac power source is applied to the Tx coil and the received power is measured at the resistive load. The transfer efficiency is defined as the ratio of input power to received power. Except for the attached 0.5-Ω-load, the rest of the settings (operating frequencies, locations of the Rx box, coil structures, medium, etc.) are identical to those of the experiment measuring effective mutual inductance.

The simulated power transmit efficiency (η) is calculated with (5) and parameters such as resistances, self-inductances, and capacitances are specified in Table II. The R^2 values are 0.99, 0.97, 0.98, and 0.97 for air, unskewed, 2-cm-skewed, and 4-cm-skewed coils for ferrite medium, respectively; thus, the calculation and measurement of the power transfer efficiency are almost consistent with those in Fig. 18.

As with the effective mutual inductance, the transfer efficiency is much higher in the system with the ferrite plate than that in the system with air. The highest efficiency through air with the unskewed Tx coil is 0.008%, whereas that with ferrite is 29.5%. Most importantly, when the distance between the coils exceeds 10 cm, no power is measured at the Rx coil with air medium. At the farthest end of the ferrite plate, the systems with the unskewed, 2-cm-skewed, and 4-cm-skewed Tx coils show 6.2%, 10.4%, and 17.5% transfer efficiencies, respectively. The highest measured transfer efficiencies are 29.5%, 33.3%, and 47.3% for the unskewed, 2-cm-skewed, and 4-cm-skewed structures on the ferrite plate, respectively.

The 4-cm-skewed coil shows the best performance as expected, and the maximum power transfer efficiency of the 4-cm-skewed ferrite system appears at 5 cm. With respect to the systems with the unskewed and 4-cm-skewed coils, the power transfer efficiency is improved up to 2.8 times at a distance of 55 cm (difference of up to 17.9% for a 5 cm distance) and two times on average (10.5% difference on average). Compared to the system with the 2-cm-skewed coil, the system with the 4-cm-skewed coil has 1.7 times higher transfer efficiency at the end of the ferrite plate (14.1% of the largest difference at 5 cm distance) and 1.4 times on average (6.2% difference on average).

Adjusting the Tx coil winding results in improved effective mutual inductance and a power transfer efficiency of as much as 17.9%, as shown in Fig. 18. The relationship between the improvement in the mutual inductance and transfer efficiency is described in Fig. 19. In both Fig. 19(a) and (b), the bars and the solid lines denote the effective mutual inductance and power transfer efficiency, respectively. The mutual inductances and transfer efficiencies at a certain distance between the transmitter and receiver are indicated in Fig. 19(a). The blue bars and solid line are the values from the system with the standard Tx coil and the red ones denote that with the adjusted Tx coil. Fig. 19(b) shows the difference between the measurement, that is the effective mutual inductance (green bar) and the power transfer efficiency (pink curve), from systems with the unskewed and skewed Tx coils. As shown in Fig. 19, especially Fig. 19(b), the tendencies for improvements in mutual inductance and transfer efficiency are consistent with each other, providing a low mean squared error (MSE) for the normalized difference, which is less than 2.8%. The result demonstrates that the design rule, namely that the enhanced mutual inductance between the Tx and Rx coils from the GBPI leads to increased power transfer efficiency of the proposed free arrangement WPT system, is valid.

D. Power Loss Analysis

Power loss analysis for the experiment in Section III for the 4-cm-skewed Tx coil system, where the receiver is located 5-cm off the Tx coil, is conducted. Fig. 20 shows each share of losses for total power. The operating power consumption of the ac power source in Fig. 7 is indicated as switching loss. The Tx and Rx coils undergo dc (conduction) loss and ac (due to skin effect and proximity effect) loss, respectively. DC resistance is calculated from resistivity of copper (which is used as the coil) and ac resistance is estimated using the ratio of ac resistance to dc resistance of the Litz wire [38]. All these losses are measured by a mixed signal oscilloscope (MSOX3034T, Keysight Technologies). It is very difficult to measure core loss when ferrite is used as the material of medium plate and the Rx box. Thus, the

TABLE III
STANDARD FOR SAFETY LEVELS WITH RESPECT TO HUMAN EXPOSURE TO ELECTRIC, MAGNETIC, AND ELECTROMAGNETIC FIELDS AT 100 KHZ

Electrostimulation effect		Thermal effect				
DRL	ERL	DRL	ERL			
Induced electric field intensity	Magnetic field intensity	Specific absorption rate	Electric field intensity	Magnetic field intensity	Power density (electric field base)	Power density (magnetic field base)
29.45 V/ m	163 A/m	0.08 W/kg	1,842 V/m	163 A/m	9,000 W/ m^2	10,000,000 W/ m^2

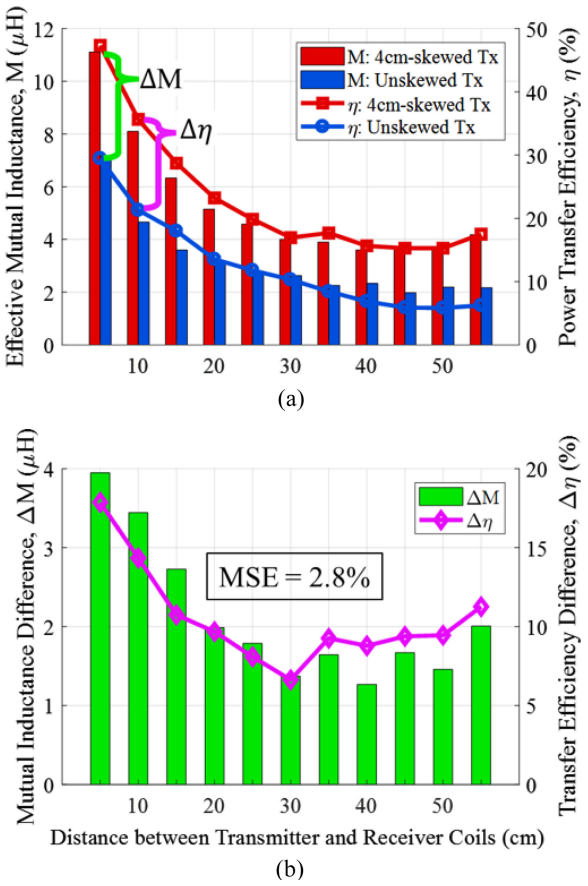

Fig. 19. Relationship of the improvements in mutual inductance and transfer efficiency through the geometric-based performance improvement method. (a) Measured mutual inductances (bars) and power transfer efficiencies (curves) according to the distance between the transmitter and receiver with the unskewed coil (blue) and the 4-cm-skewed coil (red). (b) Differences between the measurements with unskewed and skewed Tx coils in (a) and MSE.

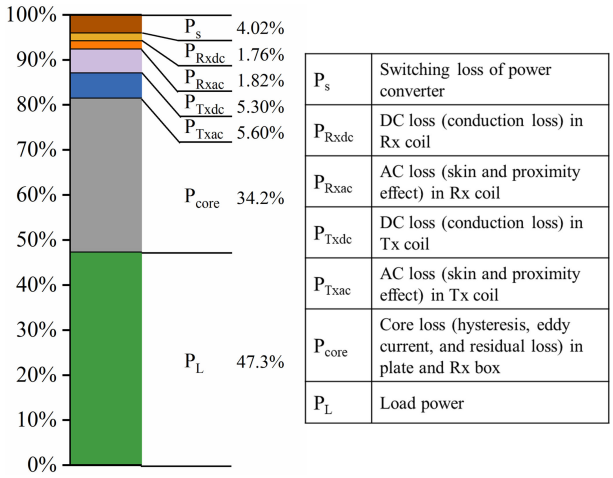

P_s	Switching loss of power converter
P_{Rxdc}	DC loss (conduction loss) in Rx coil
P_{Rxac}	AC loss (skin and proximity effect) in Rx coil
P_{Txdc}	DC loss (conduction loss) in Tx coil
P_{Txac}	AC loss (skin and proximity effect) in Tx coil
P_{core}	Core loss (hysteresis, eddy current, and residual loss) in plate and Rx box
P_L	Load power

Fig. 20. Power loss analysis on the experiment for the system with 4-cm-skewed Tx coil.

core loss is calculated using the datasheet given by the provider [39] and the relevant system value.

The values of ac loss are similar as those of dc loss since the Litz-type wire is appropriate for high frequency. The system with ferrite achieves higher efficiency (Fig. 18) but causes high and constant core loss, which is major irrespective of the location of the receiver.

E. Safety to Humans

The purpose of proposed system is to charge devices that are frequently used by humans. Thus, the system must satisfy the relevant standards for consumer electronics. Theoretically, the human body is exposed to the magnetic field after its generation and propagation by the system. We simulated propagated electric and magnetic fields of the system using FEA software and verified whether those field intensities satisfy the Standard for Safety Levels with respect to Human Exposure to Electric, Magnetic, and Electromagnetic Fields approved by IEEE [33] and guidelines provided by the International Commission on Non-ionizing Radiation Protection (ICNIRP) [29], [30]. The simulation environment is the same as the experimental setting of the 4-cm-skewed Tx coil system. In the IEEE standard, safety with regard to the electrostimulation and thermal effects should be satisfied at the operating frequency of 100 kHz used in the article. The domestic reference limit (DRL) and exposure reference limit (ERL) exist for each effect, and the system is said to be safe when the criteria fall under DRL or ERL. In this article, the proposed system complies with the DRL.

Table III shows the reference limits for the electrostimulation and thermal effects. The SAR is a measure of the rate at which energy is absorbed by the human body (units: W/kg). To obtain the SAR value, another FEA simulation application

TABLE IV
ICNIRP GUIDELINES FOR LIMITING EXPOSURE TO TIME-VARYING ELECTRIC, MAGNETIC, AND ELECTROMAGNETIC FIELDS

Guideline	Basic restrictions			Reference levels		
Criteria	Internal electric field intensity	Current density	Average SAR	Induced e lectric field intensity	Magnetic field intensity	Magnetic flux density
Low Frequency (1Hz-100kHz)	13.5 V/m	-	-	83 V/m	21A/m	27 μT
High Frequency (Up to 300GHz)	-	200 mA/ m^2	0.08 W/kg	87 V/m	5 A/m	6.25 μT

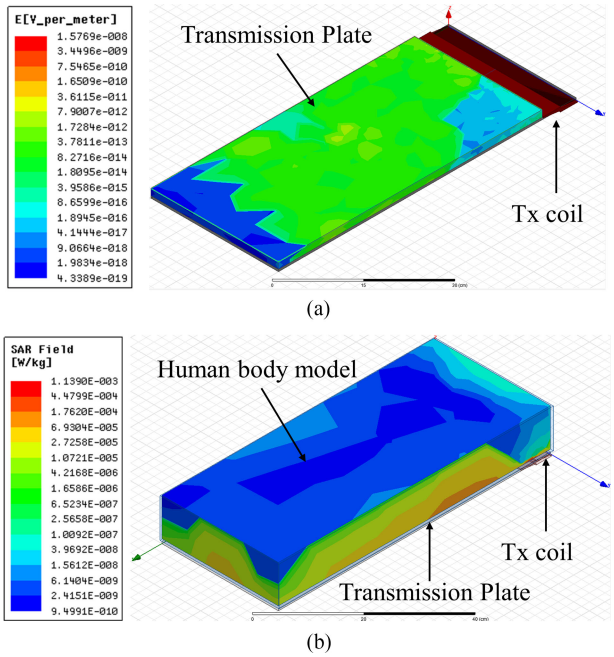

Fig. 21. Results of FEA simulation (HFSS v15.1) of the system with 4-cm-skewed Tx coil with regard to (a) electric field intensity and (b) SAR.

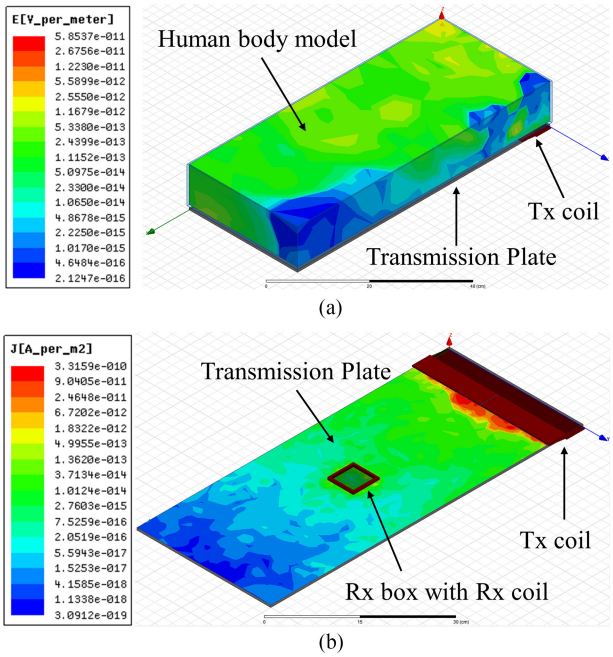

Fig. 22. Results of FEA simulation (HFSS v15.1) of the system with 4-cm-skewed Tx coil with regard to (a) internal electric field intensity and (b) surface current density.

(Ansys HFSS v15.1) is used and for other values, Ansoft Maxwell v14.0 is used to simulate the results. The box touching both the Tx coil and ferrite medium plate serves as the measurement target, i.e., the charging area.

Fig. 21(a) shows the result of the electric field intensity for electrostimulation of the system. The maximum electric field intensity is 15.77 nV/m, and thus, the system satisfies the DRL for the electrostimulation effect. Fig. 21(b) shows the SAR results for the thermal effect of the system. The brain, which is the most sensitive organ in the human body, is modeled using specific material, which is placed above the Tx coil. The simulated result for the DRL of the thermal effect is 1.14 mW/kg. Consequently, the system can satisfy the IEEE standard.

The ICNIRP guidelines for limiting exposure to time-varying electric, magnetic, and electromagnetic fields are given for low frequency (LF, 1 Hz–100 kHz) [30] and high frequency (HF, up to 300 GHz) [29]. The proposed system operates at 100 kHz; thus, the system should satisfy the guidelines for both LF and HF. Both the guideline state that the exposure fields of an electromagnetic system should be under the basic restriction or reference levels (Table IV). Compliance with the basic restriction, which is essential for the system, is verified by the simulation.

The internal electric field is the in-body electric field owing to exposure to time-varying electric and magnetic fields. In Fig. 22(a), internal electric field (0.0585 nV/m) is assessed by simulating same body model used in Fig. 21(b). Fig. 22(b) shows the results of the current density of the ferrite plate surface, where the human body can be exposed. The value for the proposed system is 0.335 nA/m^2. The SAR value as per the

TABLE V
VARIOUS PERFORMANCE COMPARISONS OF WPT SYSTEMS

Comparisons	Flexibility in alignment	Maximum distance [m]	Maximum peer-to-peer efficiency	FOM[1] (Ratio of charging area to sum of transmitter and receiver volumes) [m^{-1}]	Charging multi-receiver
Recent commercial product [2, 3]	Very low	0.003	≥ 90% at 0.003 m	N/A[2]	N/A
DCRS [24]	Moderate	5	29% at 3 m	27.8	N/A
U-ipt [27]	Very high	1	6% at 0.2 m	10	Able
Ball joint [28]	Very low	N/A	81% at 0 m	N/A	N/A
Ring resonator [16]	Low	0.7	80.1% at 0.7 m	N/A	Conditionally able
This work	High	1.3	47.3% at 0.05 m	5357	Able

[1]FOM $[\mathrm{m}^{-1}]$ $\frac{\text{Available charging area } [m^2]}{\text{Volume of transmitter}[m^3]+\text{volume of receiver}[m^3]}$
[2]N/A: Not available

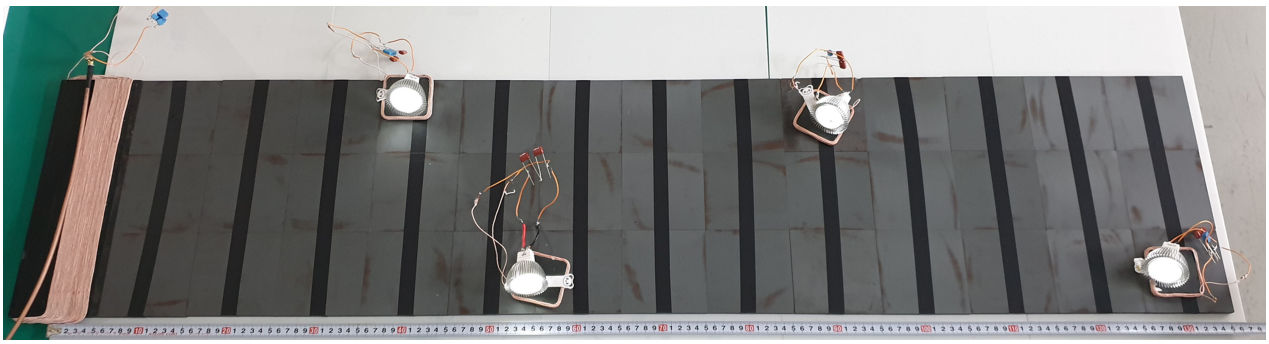

Fig. 23. Four LED bulbs are lighted with the proposed WPT system. The maximum distance of a bulb from the Tx coil is 130 cm.

ICNIRP guideline is the same as that of the IEEE standard. All criteria with respect to basic restrictions fall within the guideline. Therefore, the free arrangement WPT system satisfies the safety standards set by both the IEEE and ICNIRP as the direction of the induced magnetic field is not directed to the user.

IV. CONCLUSION

This article introduces a WPT system with ferrite in which the Rx coil can be located freely. The system employs ferrite with high permeability to achieve higher efficiency than air as the medium. While the argument of cost originates from the adaptation of the ferrite medium, properties, such as high efficiency and decreased transmitter volume deployment taking advantage of practical applications, are enough to compensate for the cost. Selecting ferrite as the medium, the plate-shaped structure of the proposed system is determined to locate the receivers without restriction and offer flexible power paths.

A coil winding structure modification is also discussed to obtain improved mutual inductance profile. The standard (unskewed Tx coil) and adjusted (2- and 4-cm-skewed Tx coils) systems are experimentally verified at 100 kHz, and show up to 29.5%, 33.3%, and 47.3% power transfer efficiency, respectively. At the longest distance of 55 cm between the Tx and Rx coils, the transfer efficiencies are 6.2%, 10.4%, and 17.5%, respectively. The 4-cm-skewed Tx coil shows the best performance, with the highest effective mutual inductance and power transfer efficiency.

The proposed structure where Tx and Rx coils are aligned at almost 90° using the ferrimagnetic material medium and adjusted Tx coil winding can be seen a combination of the horizontal and vertical flux approaches in [22]. Combining these two approaches addresses the limitations in orientation and size of the receivers as well as concerns regarding the radiated magnetic flux. Therefore, the proposed WPT system is novel in that it is flexible in terms of the placement of multiple implementable

receivers and the intensity of the magnetic field radiated to the air and absorbed by the human body is greatly reduced, dismissing the safety issue.

Several indicators from the proposed WPT system and the commercial or studied counterparts are compared in Table V to evaluate their respective performances. With regard to alignment flexibility, the proposed system achieves a high score compared to the others, indicating that the restriction on the location of receivers is highly relieved. Although the proposed system has significantly long transfer distance for the occupied volume of the transmitter, the efficiency should be improved for satisfying commercial needs. This aspect is explained in terms of figure of merit (FOM) in Table V, namely, as the ratio of available charging area to the sum of the transmitter and receiver volumes. A high FOM value means that the system obtains a larger charging area with a relatively small total volume of the Tx and Rx coils, and is more practical. Therefore, further investigations should be conducted to develop and optimize the system with respect to materials and structural adjustments. The proposed free arrangement WPT system can be installed on plate-like flat structures such as desks, floors, and walls to charge multiple mobile devices and sensors conveniently; thus, it is feasible for implementing internet of things applications.

Future Work

The large area of the charging medium plate provided in the proposed WPT system enables a receiver to be located freely on the plate and may satisfy the need to charge a multiple number of receivers, as shown in Fig. 1. Through experiments on the free arrangement WPT system, which utilize LED bulbs as loads, the possibility of using the proposed system with multiple receivers is verified.

Four receivers with the same windings, structure, and material are fabricated, and a 4–cm-skewed Tx coil with 40 turns, which showed the best performance in the simulations, is deployed for the experiment. The four bulb loads connected to each receiver are located arbitrarily on the ferrite plate of length 130 cm, as shown in Fig. 23. The other experimental settings are the same as those for measuring transfer efficiency, except for the input power. Future studies to consider multiload systems and couplings between the adjacent Rx coils should reduce the input power to light all the LED bulbs and improve the practicality of the free arrangement WPT system. Also, studies to enhance the versatility of the system, such as by reducing the weight of the plate, using flexible ferrite sheet, and optimizing the system variables, are necessary.

References

[1] N. Tesla, "System of transmission of electrical energy," U.S. Patent 645576A, 1900.

[2] Belkin. (n.d., Feb. 28, 2019). Boost Up Special Edition Wireless Charging Pad. [Online]. Available: https://www.belkin.com/kr/p/P-F7U054/

[3] Wireless Power Consortium Website. (n.d., Mar. 25, 2019). Wireless Power Standard. [Online]. Available: http://www.wirelesspowerconsortium.com

[4] A. Zaheer, G. A. Covic, and D. Kacprzak, "A bipolar pad in a 10-kHz 300-W distributed IPT system for AGV applications," *IEEE Trans. Ind. Electron.*, vol. 61, no. 7, pp. 3288–3301, Jul. 2014.

[5] S. Y. Choi, S. Y. Jeong, B. W. Gu, G. C. Lim, and C. T. Rim, "Ultraslim S-type power supply rails for roadway-powered electric vehicles," *IEEE Trans. Power Electron.*, vol. 30, no. 11, pp. 6456–6468, Nov. 2015.

[6] H. Ishida and H. Furukawa, "Wireless power transmission through concrete using circuits resonating at utility frequency of 60 Hz," *IEEE Trans. Power Electron.*, vol. 30, no. 3, pp. 1220–1229, Mar. 2015.

[7] C. C. Mi, G. Buja, S. Y. Choi, and C. T. Rim, "Modern advances in wireless power transfer systems for roadway powered electric vehicles," *IEEE Trans. Ind. Electron.*, vol. 63, no. 10, pp. 6533–6545, Oct. 2016.

[8] F. Arvin, S. Watson, A. E. Turgut, J. Espinosa, T. Krajník, and B. Lennox, "Perpetual robot swarm: Long-term autonomy of mobile robots using on-the-fly inductive charging," *J. Intell. Robot. Syst.*, vol. 92, pp 395–412, 2017.

[9] M. R. Basar, M. Y. Ahmad, J. Cho, and F. Ibrahim, "Stable and high-efficiency wireless power transfer system for robotic capsule using a modified helmholtz coil," *IEEE Trans. Ind. Electron.*, vol. 64, no. 2, pp. 1113–1122, Feb. 2017.

[10] E. S. Lee, J. S. Choi, H. S. Son, S. H. Han, and C. T. Rim, "Six degrees of freedom wide-range ubiquitous IPT for IoT by DQ magnetic field," *IEEE Trans. Power Electron.*, vol. 32, no. 11, pp. 8258–8276, Nov. 2017.

[11] Z. Li, C. Zhu, J. Jiang, K. Song, and G. Wei, "A 3-kW wireless power transfer system for sightseeing car supercapacitor charge," *IEEE Trans. Power Electron.*, vol. 32, no. 5, pp. 3301–3316, May 2017.

[12] S. C. Tang, T. L. T. Lun, Z. Guo, K.-W. Kwok, and N. J. McDannold, "Intermediate range wireless power transfer with segmented coil transmitters for implantable heart pumps," *IEEE Trans. Power Electron.*, vol. 32, no. 5, pp. 3844–3857, May 2017.

[13] Y. Jiang, L. Wang, Y. Wang, J. Liu, X. Li, and G. Ning, "Analysis, design, and implementation of accurate ZVS angle control for EV battery charging in wireless high-power transfer," *IEEE Trans. Ind. Electron.*, vol. 66, no. 5, pp. 4075–4085, May 2019.

[14] J. Xu, F. Dai, Y. Xu, C. Yao, and C. Li, "Wireless power supply technology for uniform magnetic field of intelligent greenhouse sensors," *Comput. Electron. Agriculture*, vol. 156, pp. 203–208, 2019.

[15] K. Zhang, X. Zhang, Z. Zhu, Z. Yan, B. Song, and C. C. Mi, "A new coil structure to reduce eddy current loss of WPT systems for underwater vehicles," *IEEE Trans. Veh. Technol.*, vol. 68, no. 1, pp. 245–253, Jan. 2019.

[16] W. X. Zhong, L. Chi Kwan, and S. Y. Hui, "Wireless power domino-resonator systems with noncoaxial axes and circular structures," *IEEE Trans. Power Electron.*, vol. 27, no. 11, pp. 4750–4762, Nov. 2012.

[17] D. Liu, H. Hu, and S. V. Georgakopoulos, "Misalignment sensitivity of strongly coupled wireless power transfer systems," *IEEE Trans. Power Electron.*, vol. 32, no. 7, pp. 5509–5519, Jul. 2017.

[18] Z. Zhang, H. Pang, A. Georgiadis, and C. Cecati, "Wireless power transfer - An overview," *IEEE Trans. Ind. Electron.*, vol. 66, no. 2, pp. 1044–1058, Feb. 2019.

[19] A. Kurs, A. Karalis, R. Moffatt, J. D. Joannopoulos, P. Fisher, and M. Soljačić, "Wireless power transfer via strongly coupled magnetic resonances," *Science*, vol. 317, no. 5834, pp. 83–86, 2007, doi: 10.1126/science.1143254.

[20] F. Zhang, S. A. Hackworth, F. Weinong, and M. Sun, "The relay effect on wireless power transfer using witricity," in *Proc. Dig. 14th Biennial IEEE Conf. Electromagn. Field Comput.*, May 9–12, 2010.

[21] A. Noda and H. Shinoda, "Selective wireless power transmission through high-Q flat waveguide-ring resonator on 2-D waveguide sheet," *IEEE Trans. Microw. Theory Techn.*, vol. 59, no. 8, pp. 2158–2167, Aug. 2011.

[22] S. Y. Hui, "Planar wireless charging technology for portable electronic products and Qi," *Proc. IEEE*, vol. 101, no. 6, pp. 1290–1301, Jun. 2013.

[23] S. K. Oruganti, S. H. Heo, F. Bien, and H. Ma, "Wireless energy transfer-based transceiver systems for power and/or high-data rate transmission through thick metal walls using sheet-like waveguides," *Electron. Lett.*, vol. 50, no. 12, pp. 886–888, 2014.

[24] C. Park, S. Lee, G.-H. Cho, and C. T. Rim, "Innovative 5-m-off-distance inductive power transfer systems with optimally shaped dipole coils," *IEEE Trans. Power Electron.*, vol. 30, no. 2, pp. 817–827, Feb. 2015.

[25] W. X. Zhong, C. Zhang, X. Liu, and S. Y. R. Hui, "A methodology for making a three-coil wireless power transfer system more energy efficient than a two-coil counterpart for extended transfer distance," *IEEE Trans. Power Electron.*, vol. 30, no. 2, pp. 933–942, Feb. 2015.

[26] X. Y. Zhang, C. Xue, and J. Lin, "Distance-insensitive wireless power transfer using mixed electric and magnetic coupling for frequency splitting suppression," *IEEE Trans. Microw. Theory Techn.*, vol. 65, no. 11, pp. 4307–4316, Nov. 2017.

[27] B. G. Choi, Y.-H. Sohn, E. S. Lee, S. H. Han, H. R. Kim, and C. T. Rim, "Coreless transmitting coils with conductive magnetic shield for wide-range ubiquitous IPT," *IEEE Trans. Power Electron.*, vol. 34, no. 3, pp. 2539–2552, Mar. 2019.
[28] C. Zhang, D. Lin, and S. Y. R. Hui, "Ball-joint wireless power transfer systems," *IEEE Trans. Power Electron.*, vol. 33, no. 1, pp. 65–72, Jan. 2018.
[29] J. Herbertz, "Comment on the ICNIRP guidelines for limiting exposure to time-varying electric, magnetic, and electromagnetic fields (up to 300 GHz)," *Health Phys.*, vol. 75, no. 5, pp. 493–511, Nov. 1998.
[30] International Commission on Non-Ionizing Radiation Protection, "Guidelines for limiting exposure to time-varying electric and magnetic fields (1 Hz to 100 kHz)," *Health Phys.*, vol. 99, no. 6, pp. 818–836, Dec. 2010.
[31] A. Christ *et al.*, "Evaluation of wireless resonant power transfer systems with human electromagnetic exposure limits," *IEEE Trans. Electromagn. Compat.*, vol. 55, no. 2, pp. 265–274, Apr. 2013.
[32] Y. Zhang and M. A. D. Rooij, "How eGaN® FETs are enabling large area wireless power transfer," in *Proc. 2017 IEEE 5th Workshop Wide Bandgap Power Devices Appl.*, 2017, pp. 366–372.
[33] *PC95.1™/D3.5 draft standard for safety levels with respect to human exposure to electric, magnetic and electromagnetic fields, 0 Hz to 300 GHz*, IEEE-SA Standards Board, pp. 1–62, 2018.
[34] M. K. Kazimierczuk, G. Sancineto, G. Grandi, U. Reggiani, and A. Massarini, "High-frequency small-signal model of ferrite core inductors," *IEEE Trans. Magn.*, vol. 35, no. 5, pp. 4185–4191, Sep. 1999.
[35] R. G. D. Steel and J. H. Torrie, *Principles and Procedures of Statistics, With Special Reference to the Biological Sciences*. New York, NY, USA: McGraw-Hill, 1960, pp. 183–193.
[36] S. M. Ross, *Introduction to Probability and Statistics for Engineers and Scientists*, 5th ed. Amsterdam, The Netherlands, Boston, MA, USA: Elsevier, AP, 2014, pp. 376–378.
[37] C. L. W. Sonntag, E. A. Lomonova, and J. L. Duarte, "Implementation of the Neumann formula for calculating the mutual inductance between planar PCB inductors," in *Proc. 18th Int. Conf. Elect. Mach.*, Sep. 6–9, 2008.
[38] New England Wire. (n.d., Jun. 12, 2019). Traditional Litz Wire Theory. [Online]. Available: https://www.newenglandwire.com/traditional-litz-wire-theory/
[39] Samwha Electronics. (n.d., Jul. 26, 2018). Material Characteristics of SN-20. [Online]. Available: http://www.samwha.co.kr/electronics/product/product_ferrite_mat.aspx

Seoktae Seo received the B.S. degrees in electrical engineering from the Ulsan National Institute of Science and Technology (UNIST), Ulsan, Korea, in 2016. He is currently working toward the M.S. and Ph.D. combined degree with the UNIST.

He has worked on developing wireless power transfer system. His current research interests include wireless power transfer system and biosensors.

Hyunkyeong Jo (S'19) received the B.S. degree in mechanical engineering from the Ulsan National Institute of Science and Technology (UNIST), Ulsan, Korea, in 2016. She is currently working toward the M.S. and Ph.D. combined degree in electrical engineering with the UNIST.

She has worked on developing wireless power transfer system. Her current research interests include wireless power transfer system and metamaterial.

Franklin Bien (M'03–SM'14) received the B.S. degree in electronics engineering from Yonsei University, Seoul, South Korea, in 1997, and the M.S. and Ph.D. degrees in electrical and computer engineering from the Georgia Institute of Technology, Atlanta, GA, USA, in 2000 and 2006, respectively.

He was with Agilent Technologies and Quellan, Inc. He was also with Staccato Communications, San Diego, CA, USA, as a Senior IC Design Engineer working on analog/mixed-signal IC and RF front-end blocks for ultrawideband (UWB) products such as wireless-USB in 65-nm CMOS technologies. Since 2009, he has been a Professor with the School of Electrical and Computer Engineering, the Ulsan National Institute of Science and Technology (UNIST), Ulsan, South Korea. In an early stage of his career, his research interests included signal integrity improvement with crosstalk noise cancellation, equalization techniques for 10+ Gb/s broadband communication applications, CMOS RF front-end circuits for wireless communications and automotive radar circuits, and adaptive circuits for wireless power transfer (WPT) applications. All of these previous endeavors are migrating in the biomedical IT research direction to form his current research interests. Multitarget radar technology is moving toward respiratory detecting radar, touch screen panel drive IC and readout IC research is migrating toward biosignature/finger print detectors, and wireless power transfer research is actively being applied to medically implantable devices such as capsule endoscopy, pace makers, cortisol sensors, and in *vivo* continuous glucose monitoring systems.